First-Principles Study of Structural, Elastic, Electronic and Optical Properties of Zinc Ferrite Spinel

IOP Conf. Series: Materials Science and Engineering **569** (2019) 022016 doi:10.1088/1757-899X/569/2/022016

First-Principles Study of Structural, Elastic, Electronic and Optical Properties of Zinc Ferrite Spinel

Yifeng Meng[1], Weimei Shi[1, 2], Chao Lu[1], Shiqing Yang[1], Qingxue Yang[1], J. G. Deng[3]

[1] Chengdu Polytechnic, Chengdu, 610041, P. R. China

[2] Sichuan University, Chengdu, 610065, P. R. China

[3] China Academy of Engineering Physics, Mianyang, 621900, P. R. China

[1]Yifeng Meng:mengyifeng@163.com

Abstract: Structural, electronic,elastic and optical properties of ternary spinel oxides ZnFe2O4 have been studied by using first-principles calculation. The results show that all elastic constants are consistent with the mechanical stability criteria for cubic crystals, which indicated that ternary spinel oxides ZnFe2O4 are mechanically stable. The perfect spinel ZFO has the properties of direct bandgap semiconductor, which decreases with the increase of pressure.The DOS and Mulliken overall analysis shows that the Zn-O bonds and Fe-O bonds are covalent, and the Zn-O bond is stronger than the Fe-O bond. The results of the calculation show that the optical properties are in good agreement with the recent experimental results.

1. Introduction

Spinel structure is the important structures for AB2O4 compounds, which is cubic and has Fd-3m space group.In formula AB_2O_4, A is a cation with +2 charges and B is a cation with +3 charges, and oxygen atoms have cubic close-packed arrangement. Zinc ferrite ($ZnFe_2O_4$, shorted as ZFO hereafter) has obtained great attention due to its excellent properties in many fields, such as photocatalysis[1], application in energy storage[2], electronics[3]. TiO2 is one of the most popular photocatalysts, however, with a band gap of 3.20 eV, it can only absorb about 4% of solar energy. The band gap of ZFO is 1.90ev, which is relatively narrow and much smaller than that of TiO2.Hence, ZFO could absorb a larger percentage of solar energy in visible-light region, which makes ZFO an attractive candidate for photocatalysis. ZFO not only has photocatalytic effect, but also is an important anode material in energy storage technology due to its non-toxic, abundant earth resources and large specific capacity. Jia *et al.* successfully synthesized a ZFO anode material, which displayed a stable capacity of 1091 mAh/g for 190 cycles at a medium de-lithiation potential of 1.7 V[4]. Vadiyar *et al.* prepared the ZFO/NRG composite *via* a facile solvothermal strategy followed by calcining treatment for high-performance supercapacitor electrode. The ZFO/NRG showed favorably electrical performance including specific capacitance, rate capability and cycling performance[5]. In addition, by using co-precipitation method, Vinosha *et al.* synthesized highly crystalline, single phase spinel ZFO nanoparticles with small particle size and favorable magnetic properties, which is a fitting candidate in the field of electronics[6].

Compared to numerous experimental investigations[7-14], there are also a few literatures refer to theoretical study. For example, Yao *et al.* investigated the electronic structures and stability of In-substituted ZFO by first-principles calculation using a GGA/RPBE scheme[7]. After two years, by

using the same method, Yao et al. studied the geometric and electronic structures of ZFO with various vacancy defects[8].

In the present paper, the structural, electronic, elastic and optical properties of zinc ferrite with spinel structure at 0 GPa, 11 GPa and 23 GPa were studied by using first-principles calculations, in which the generalized gradient approximation (GGA) and Hubbard U approach was employed to describe the on-site Coulomb interactions in the localized d orbital of Fe atoms in ZFO.

2 .Computational details

All the spin-polarized density functional calculations were carried out by using Cambridge Serial Total Energy Package (CASTEP)[9, 10]program, which uses a total energy plane wave pseudopotential method[11]. The Perdew-Burke-Ernzerhof (PBE)[12] function within the generalized gradient approximation (GGA) was employed to describe the exchange and correlation interaction among electrons. The plane-wave basis set was restricted by a cutoff energy of 500 eV. A 3×3×3 Monkhorst-Pack grid[13] was used for integration over the irreducible part of the Brillouin zone of the supercells. The convergence criterion of the largest force on atoms was 0.03 eV/Å, and the self-consistent convergence accuracy was set at 1×10^{-5} eV/atom, respectively.

TThe GGA+U method introduces an intra-atomic electron-electron interaction as an on-site correction to describe systems with f electrons and localized d. To well interpret the strong correlated interactions of the iron d orbitals, a moderate on-site Coulomb repulsion U = 5.0 eV was used. When a Hubbard U correct the iron d orbitals with 5.0 eV, the DFT-optimized lattice parameter (8.52 Å) is consistent with the value measured experimentally. The pressure is applied by the equivalent hydrostatic pressure.

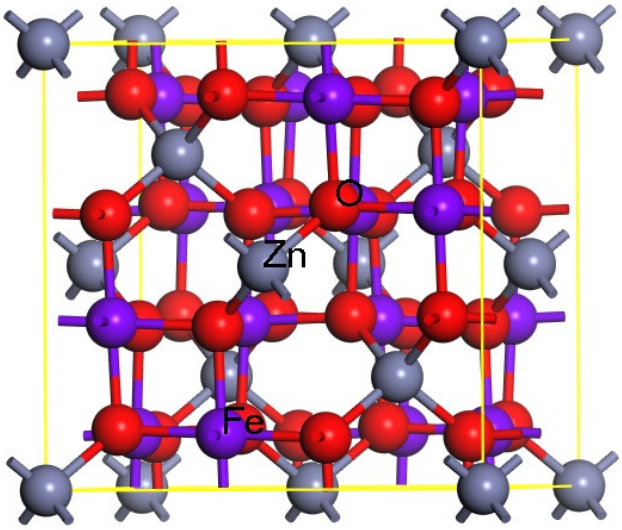

Figure 1 The spinel structure of ZFO. Grey, purple and red balls represent Zn, Fe and O atoms, respectively.

3. Results and discussion

3.1 structural properties

The normal spinel ZFO is a close packed face-centered-cubic structure with space group of Fd-3m and there are eight formula units in the unit cell, as shown in Figure 1. The calculated lattice parameters of spinel ZFO at different pressures were shown in Table 1, and it is found that the calculated lattice value of 8.52 Å at 0 GPa is consistent with experimental lattice value of 8.52 Å[14].With increasing pressure, the lattice parameters decrease from 8.52 Å to 8.33 Å at 11 GPa and 8.18 Å at 23 GPa. The calculated bond lengths of Zn – O, Fe – O and O – O also are shown in Table 1, they decrease with the

pressure increasing.

Table 1 Calculated lattice parameters (a, in Å), Mulliken atomic charge population (e), Mulliken overlap population of bonds and related bond lengths (Å)

	a	atom	charge	bond	population	bond length
		Zn	1.06	Zn–O	0.36	2.00
0 GPa	8.52	Fe	0.89	Fe–O	0.28	2.04
		O	–0.71	O–O	–0.03	2.76
		Zn	1.08	Zn–O	0.39	1.95
11 GPa	8.33	Fe	0.88	Fe–O	0.28	2.00
		O	–0.71	O–O	–0.03	2.71
		Zn	1.10	Zn–O	0.41	1.90
23 GPa	8.18	Fe	0.87	Fe–O	0.28	1.97
		O	–0.71	O–O	–0.03	2.67

3.2 Elastic properties

For cubic crystal system, the elastic modulus matrix can be written as follows:

$$\left[C_{ij}\right] = \begin{bmatrix} C_{11} & C_{12} & C_{12} & 0 & 0 & 0 \\ C_{12} & C_{11} & C_{12} & 0 & 0 & 0 \\ C_{12} & C_{12} & C_{11} & 0 & 0 & 0 \\ 0 & 0 & 0 & C_{44} & 0 & 0 \\ 0 & 0 & 0 & 0 & C_{44} & 0 \\ 0 & 0 & 0 & 0 & 0 & C_{44} \end{bmatrix}$$

Obviously, a cubic crystal has only three different elastic constants C_{11}, C_{12} and C_{44} (listed in Table 2), and all elastic constants satisfy the well-known mechanical stability criteria[15] given by

$$C_{11} > 0, C_{44} > 0, C_{11} > \left|C_{12}\right|, (C_{11} + 2C_{12}) > 0. \quad (1)$$

It means that all the investigated spinel structures are mechanically stable. In order to further investigate the mechanical properties of the zinc ferrite, the bulk modulus (B) and shear modulus (G) can be obtained from the calculated elastic constants by using Voigt-Reuss-Hill averaging scheme[16]. Young's modulus (E) and Poisson' ration (ν) can be calculated by the following equations:

$$E = \frac{9BG}{3B + G} \quad (2)$$

$$\nu = \frac{3B - 2G}{2(3B + G)} \quad (3)$$

The Zener anisotropic factor (A) can be calculated by using the following relation[17]:

$$A = \frac{2C_{44}}{(C_{11} - C_{12})} \quad (4)$$

All calculated values of elastic properties for spinel ZFO are given in Table 2.

Table 2 Calculated elastic constants (C_{11}, C_{12} and C_{44}, in GPa), bulk modulus (B, in GPa), shear modulus (G, in GPa), Young's modulus (E, in GPa), Poisson's ration (ν), Pugh's ratio (B/G) and anisotropic factor (A) under various pressure for ZFO

ZFO	C_{11}	C_{12}	C_{44}	B	G	E	ν	B/G	A
0 GPa	219.20	145.84	81.36	170.30	59.10	158.91	0.34	2.88	2.22
11 GPa	210.60	132.52	58.40	158.55	49.69	134.98	0.36	3.19	1.50
23 GPa	232.72	193.76	58.97	206.74	37.87	107.07	0.41	5.46	3.03

For ZFO under various pressures, $B > G$, which demonstrates that the shear modulus is the

parameter that limits the mechanical stability. The Young's modulus *E* is an important parameter which is defined as the ratio of the tensile stress to the tensile strain[18].It is used to measure the stiffness of the solid. The higher the value of the Young's modulus E, the stiffer is the material. From Table 2, it can be found that the calculated Young's modulus E decreases with increasing pressure, indicating that The pressure has a great influence on the stiffness of ZFO, and the stiffness is inversely proportional to the pressure. The stability of the material is reflected by the Poisson's ratio.The Poisson's ratio is proportional to the plasticity of materials.Additionally, Poisson's ratio provides useful information about the characteristic of the bonding forces; Nye reported that the upper and lower values of Poisson's ratio for central force solid are 0.50 and 0.25, respectively[19]. The Poisson's ratios calculated in this paper are higher than the lower limit value of 0.25, indicating that that the interatomic force in ZFO is central force.Pugh's ratio *B/G* is one of the most widely used empirical criterion to distinguish the ductile and brittle behavior of a material[25]. If B/G > 1.75, the material behaves as ductile, whereas if B/G < 1.75, the material behaves as brittle. In this study, the value of B/G is higher than 1.75, indicating ZFO is ductile at 0 GPa, 11 GPa and 23 GPa. With respect to A, the material is elastically isotropic when A is equal to one, otherwise it is elastically anisotropic. The present calculated Zener anisotropy factors for ZFO at various pressures indicate that ZFO is not an elastic isotropic material.

3.3 Electronic properties

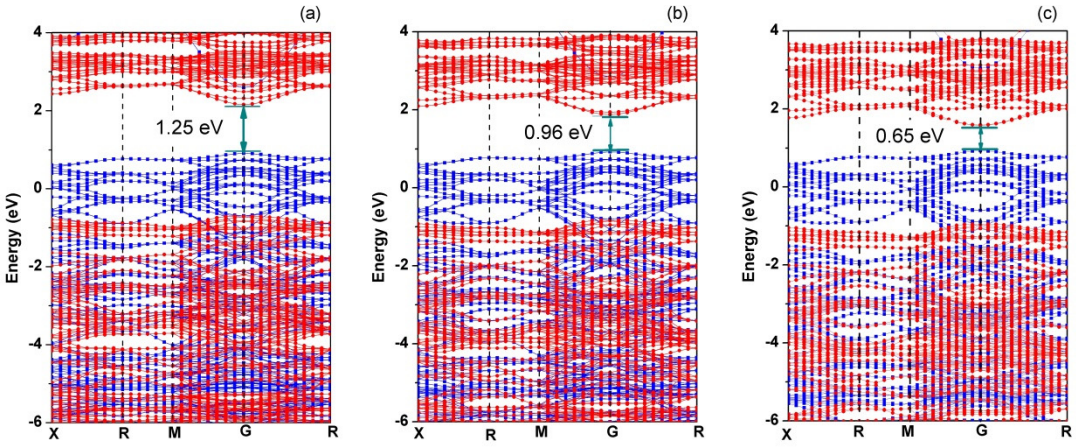

Figure 2 The band structure of ZFO at 0 GPa (a), at 11 GPa (b) and at 23 GPa (c) with horizontal dark cyan lines indicate the energy positions of the VBM and CBM.

The calculated band structure along high symmetry directions in the Brillouin zone of ZFO is shown in Figure 2, it clearly shows that the perfect spinel ZFO is a direct-gap semiconductor with a band gap of 1.25 eV. The VBM dispersion characteristic of ZFO is very flat, which leads to large holes with large effective mass and poor p-type conductivity. Obviously, the band gap decreases with increasing pressure, which is 0.96 eV at 11 GPa and 0.65 eV at 23 GPa, just as a number of compounds, $ZnAl_2S_4$[20], $MnIn_2S_4$[21], BN nanotubes[22]. The reason for such a phenomenon can be attributed to a high covalency of chemical bond, or significant re-distribution of electron density[23]. With increasing pressure, the crystal volume decreases to some extent. Simultaneously, the interatomic distance and bond-length decreases (Table 1), which improves electron common movement and induce a high covalency.

Figure 3 shows the calculated spin-polarized total density of states (TDOS) and partial density of states (PDOS) within the GGA+U framework of ZFO, which gives contributions of different atomic orbitals in the electronic band structure. The position of the Fermi energy level is indicated by the the dashed vertical line,and the Fermi energy level corresponds to the energy of zero. Clearly seen from Figure 3, the density of states near Fermi level is consists of Fe 3d state and O 2p state. Moreover, the

3d orbital (electrons) of Fe are the primary contributor to conduction band minimum (CBM), the 3d of Fe and 2p of O are the main contributor to valence band maximum (VBM), which indicates that there exists a covalence bond character between Fe and O atoms. With respect to Zn atoms, 3d state of Zn atoms strongly hybridized with 2p state of O atoms in energy region of about −9.0 ~ −1 eV (in lower valence band). More importantly, in energy region of about 5 ~ 10 eV, 4s and 4p states of Zn atoms appear, which indicates that Zn atom bond with O atoms in the form of sp^3 hybridization and form a stable covalent bond. These results are consistent with the results of Mulliken population in Table 1 and the previous study of Yao[15], [16]*et al*.

It is well-known that a high value of the bond population indicates a covalent bond, whereas a low value denotes the ionic bonds. A value of zero indicates a perfectly ionic bond and the values greater than zero indicate the increasing levels of covalency[24]. In Table 1, the Mulliken overlap populations of Zn–O bond are 0.36, 0.39 and 0.41 at pressure of 0 GPa, 11 and 23 GPa, respectively. The results indicate that Zn–O bond has a covalent character, and the strength is stronger and stronger with increasing pressure. It can be found that Fe–O bond is also covalent bond, and the strength has no change with increasing pressure.

With increasing pressure, the shapes of the peaks of DOS have no obvious changes. The results show that there is no obvious change in the structure of ZFO and no structural phase transformation under the condition of pressure less than 23 GPa.Additionally, conduction band and valence band broaden slightly with increasing pressure, which could improve the mobility of photo-generated electrons and holes. Further, the photocatalytic activity of ZFO could be improved.

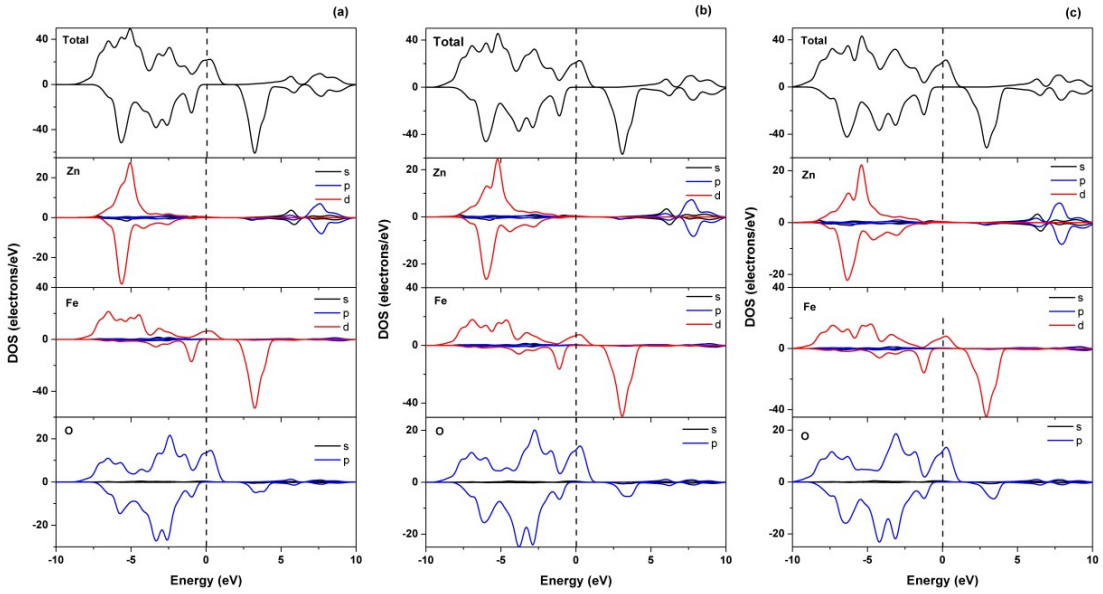

Figure 3 The calculated partial density of states of ZFO at (a) 0 GPa, (b) 11 GPa and (c) 23 GPa. The vertical dashed line at zero energy level indicates the Fermi level.

3.4 Optical properties

In this present paper, the band gap is underestimated in some extent, a “scissors operator” of 0.65 eV is used to calculate optical properties, which allowing a shift of the bands situated above the valence band and a rescaling of the matrix elements. The complex dielectric function is one of the main optical characteristics of a solid, which is given by $\varepsilon(\omega) = \varepsilon_1(\omega) + i\varepsilon_2(\omega)$. In CASTEP, the imaginary part $\varepsilon_2(\omega)$ of dielectric function is calculated numerically by adding direct evaluation of the matrix elements between the occupied and unoccupied electronic states, the real part $\varepsilon_1(\omega)$ is calculated by using the Kramers-Kroning relationship[25]. Figure 4 shows the real and imaginary parts of the dielectric functions up to 15 eV, simply because the real and the imaginary parts of spinel ZFO are nearly

constant after 15 eV. It can be seen that the first optical critical point of the real part appears at about 0.6ev, and then rapidly drops to 1.17ev. Further increase the frequency, the value of $\varepsilon 1(\omega)$ increases slowly and up to a constant of 0.80. For the imaginary part of the dielectric function, the first peak appears around 0.8 eV, and then gradually decreases to zero around 15 eV. Generally, when absorption starts, $\varepsilon 2(\omega)$ is nonzero. Therefore, ZFO becomes transparent above 15 eV. As a result, ZFO becomes transparent above 15ev.The value of the static dielectric constant of ZFO is 33.5, which indicates that ZFO is a promising dielectric material.

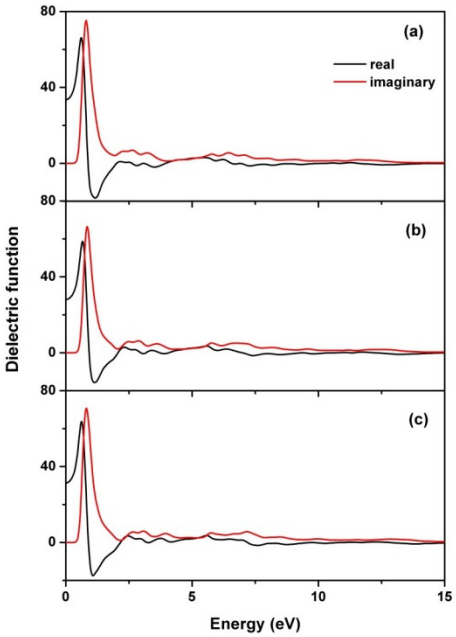

Figure 4 Real and imaginary parts of the complex dielectric function of ZFO in spinel structure at (a) 0 GPa, (b) 11 GPa and (c) 23 GPa.

Correspondingly, Figure 5 shows the calculated absorption spectra of ZFO in the polycrystalline sample, which indicated the prominent absorption band occurs in UV region. Meanwhile, ZFO also shows absorption bands in visible region. The results are in agreement with experimental results[26].

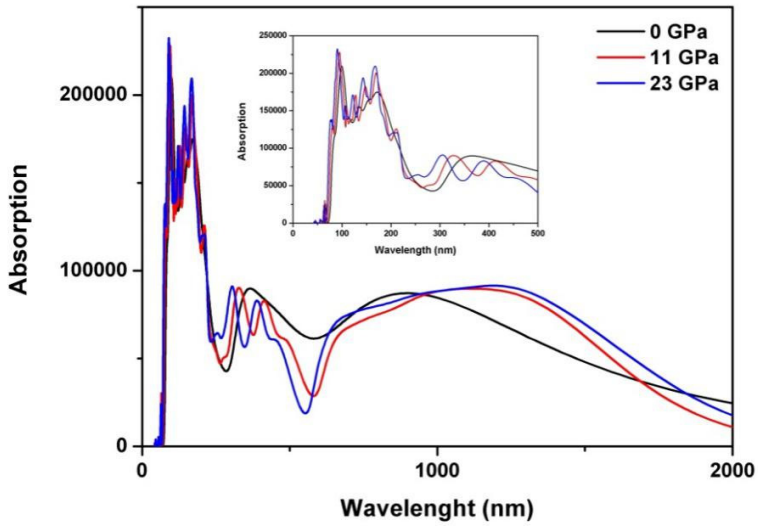

Figure 5 The absorption spectra of ZFO in spinel structure.

4. Conclusions

In this paper, the structural, elastic, electronic and optical properties of ZFO in spinel structure at different pressure were studied using DFT, which was performed using the CASTEP module of Materials Studio package. It is obtained that ZFO satisfy the well-known requirements of mechanical stability for cubic crystals. The lattice constant and band gap decrease with pressure. The calculated DOS and Mulliken population results are consistent with previous reports[15],[16]. The optical properties have also been calculated, the results are in agreement with experimental results.

Acknowledgement

This work was financially supported by the Youth Foundation of Chengdu Polytechnic （No.:15CZY29）, Research Fund of Sichuan Provincial Department of Education (No.: 18ZB0181), 3D-printing Science and Technology Innovation Team (No.: 16CZYTD446) .

References

[1] P. H. Borse, J. S. Jang, S. J. Hong, J. S. Lee, J. H. Jung, T. E. Hong, C. W. Ahn, E. D. Jeong, K. S. Hong, J. H. Yoon and H. G. Kim, Photocatalytic Hydrogen Generation from Water-methanol Mixtures Using Nanocrystalline $ZnFe_2O_4$ under Visible Light Irradiation, Journal of the Korean Physical Society, 55 (4), 1472-1477, 2009

[2] Yan-Na NuLi, Yan-Qiu Chu and Qi-Zong Qin, Nanocrystalline $ZnFe_2O_4$ and Ag-Doped $ZnFe_2O_4$ Films Used as New Anode Materials for Li-ion Batteries, J. Electrochem. Soc, 151,A1077-A1083, 2004

[3] U. S. Sharma, Ram Naresh Sharma, Rashmi Shah, Study of physical and magnetic properties of zinc ferrite nanoparticles, Quantum Matter, 5 (3), 423-425, 2016

[4] Haiping Jia, Richard Kloepsch, Xin He, Marco Evertz, Sascha Nowak, Jie Li, Martin Winter and Tobias Placke, Nanostructured $ZnFe_2O_4$ as anode material for lithium-ion batteries: ionic liquid- assisted synthesis and performance evaluation with special emphasis on comparative metal dissolution, Acta Chim. Slov. 2016, 63, 470-483

[5] Lei Li, Huiting Bi, Shili Gai, Fei He, Peng Gao, Yunlu Dai, Xitian Zhang, Dan Yang, Milin Zhang and Piaoping Yang, Uniformly dispersed $ZnFe_2O_4$ nanoparticles on nitrogen-modified graphene for high-performance supercapacitor as electrode, Sci. Rep., 2017, 7, 43116

[6] P. Annie Vinosha, L. Ansel Mely, J. Emima Jeronsia, F. Heartlin Monica, K. Raja, S. Jerome Das,

Study of Structural, optical, dielectric and magnetic properties of zinc ferrite synthesized by co- precipitation, Nano Hybrids and Composites, 17, 1-9, 2017
[7] Jinhuan Yao, Yanwei Li, Xuanhai Li and Shiru Le, First-principles investigation on the electronic structure and stability of In-substituted $ZnFe_2O_4$, Metallurgical and Materials Transactions A, 45A, 3686-3693, 2014
[8] Jinhuan Yao, Yanwei Li, Xuanhai Li and Xiaodong Zhu, First-principles study of the geometric and electronic structures of zinc ferrite with vacancy defect, 47A, 3753-3760, 2016
[9] M. D. Segall, P. J. D. Lindan, M. J. Probert, C. J. Pickard, P. J. Hasnip, S. J. Clark, and M. C. Payne, First-principles simulation: ideas, illustrations and the CASTEP code, J. Phys.: Condens. Matter, 2002, 14 (11), 2717-44
[10] Stewart J. Clark, Matthew D. Segall, Chris J. Pickard, Phil J. Hasnip, Matt I. J. Probert, Keith Refson and Mike C. Payne, First principles methods using CASTEP, Zeitschrift fuer Kristallographie, 220(5-6), 2005, 567-570
[11] M. C. Payne, M. P. Teter, D. C. Allan, T. A. Arias, J. D. Joannopoulos, Iterative minimization techniques for ab initio total-energy calculations: molecular dynamics and conjugate gradients, Rev. Mod. Phys., 1992, 64, 1045
[12] John P. Perdew, Kieron Burke, Matthias Ernzerhof, Generalized gradient approximation made simple, Phys. Rev. Lett., 1996, 77, 3865
[13] Hendrik J. Monkhorst, James D. Pack, Special points for Brillouin-zone integrations, Phys. Rev. B, 1976, 13, 5188
[14] K. Kamazawa, Y. Tsunoda, K. Odaka, K. Kohn, Spin liquid state in $ZnFe_2O_4$, J. Phys. Chem. Solids, 1999, 60, 1261-1264 Y. Yamada, K. Kamazawa, Y. Tsunoda, Interspin interactions in $ZnFe_2O_4$: Theoretical analysis of neutron scattering study, Phys. Rev. B., 2002, 66, 064401 K. Kamazawa, Y. Tsunoda, H. Kadowaki, K. Kohn, Magnetic neutron scattering measurements on a single crystal of frustrated $ZnFe_2O_4$, Phys. Rev. B., 2003, 68, 024412
[15] Zhi-jian Wu, Er-jun Zhao, Hong-ping Xiang, Xian-feng Hao, Xiao-juan Liu, and Jian Meng, Crystal structures and elastic properties of superhard IrN_2 and IrN_3 from first principles, Physical Review B, 76, 054115, 2007
[16] R. Hill, The elastic behaviour of a crystalline aggregate, Proceedings of the Physical Society A, 1952, 65, 349-354
[17] D. G. Pettifor, Theoretical predictions of structure and related properties of intermetallics, Mater. Sci. Technol., 1992, 8, 345
[18] S. F. Pugh, Relations between the elastic moduli and the plastic properties of polycrystalline pure metals, Philos. Mag., 1954, 45, 823
[19] J. F. Nye, Properties Physiques des Materiaux, Dunod, Paris, 1961
[20] M. G. Brik, First-principles calculations of electronic, optical and elastic properties of $ZnAl_2S_4$ and $ZnGa_2O_4$, Journal of Physics and Chemistry of Solids, 2010, 71, 1435-1442
[21] J. Ruiz-Fuertes, D. Errandonea, F. J. Manjon, D. Martinez-Garcia, A. Segura, V. V. Ursaki, I. M. Tiginyanu, High-pressure effects on the optical-absorption edge of $CdIn_2S_4$, $MgIn_2S_4$, and $MnIn_2S_4$ thiospinels, J. Appl. Phys., 2008, 103, 063710
[22] S. S. Coutinho, V. Lemos, S. Guerini, Band-gap tenability of a (6, 0) BN nanotube bundle under pressure: Ab initio calculations, Phys. Rev. B, 2009, 80, 193408
[23] Zhang Hong, Tang Jin, Cheng Xin-Lu, Structural, electronic properties and chemical bonding of borate $Li_4CaB_2O_6$ under high pressure: an Ab initio investigation, Chin. Phys. Lett., 2008, 25, 552
[24] M. D. Segall, Rajiv Shah, Chris J. Pickard, M. C. Payne, Population analysis of plane-wave electronic structure calculation of bulk materials, Phys. Rev. B, 1996, 23, 16317-16320
[25] J. S. Toll, Causality and the dispersion relation: logical foundations, Phys. Rev., 1956, 104, 1760-1770
[26] R. C. Sripriya, Ezhil Arasi S., Madhavan J., Victor Antony Raj M., Synthesis and Charecterization studies of $ZnFe_2O_4$ nanoparticles, Mechanics, Materials Science & Engineering, 2017, 9 (1)